Aeromagnetic and Magnetotelluric Studies in Guaribas Region of Parnaiba Basin in North East Brazil for Groundwater Assessment

E. Chandrasekhar[1], Mita Rajaram[2], S.P. Anand[2], Sergio L. Fontes[3] and Jean Marie Flexor[3]
[1]Department of Earth Sciences, Indian Institute of Technology Bombay, Powai, Mumbai-400 076, India; esekhar@iitb.ac.in
[2]Indian Institute of Geomagnetism, Kalamboli, New Panvel, Navi Mumbai, 410 218, India, mita@iigs.iigm.res.in
[3]Departamento de Geofisica, Observatorio Nacional – MCT, Rio de Janeiro, CEP 20921-400, RJ Brazil, sergio@on.br

This paper was prepared for presentation at the 9th International Congress of the Brazilian Geophysical Society held in Salvador, Brazil, 11-14 September 2005.

Abstract

Aeromagnetic and Magnetotelluric (MT) surveys have been conducted over the intra cratonic sedimentary Parnaiba basin located in the semi-arid northeastern part of Brazil for sub-surface structural mapping and ground water resource investigation. From aeromagnetic data several faults in the sub-surface have been identified that are conducive to be potential groundwater resource regions. Broad band (0.001sec – 1000sec) MT soundings along a profile within the area surveyed aeromagnetically, mapped two localized high conductivity zones (of resistivities <10 Ω-m) representing sedimentary aquifer zones. These zones lie close to the faults identified from the aeromagnetic survey whose top lies at depth of 150m.

Introduction

The Parnaiba basin in NE Brazil is oval in shape and spans the entire region by about 1000km in NW and by about 800km in SE. Its evolutionary history and shape are controlled by the Trans-Brazilian Lineament, which is composed of small-scale faults and dykes that cut geological units of distinct periods and is related to several basement grabens found at both NE and SW ends of the basin. (Cunha, 1986). The basin is very thin and is mainly composed of Paleozoic sediments of Serra Grande and Caninde groups of Silurian and Devonian. The lithology in the East and SE margins (the present study region) of the Parnaiba basin is mainly composed of shales, siltstones, coarse-to-fine sandstones, conglomerates, quartz pebbles etc (see Fig.2 of Meju et al, 1999 for more lithological details). Several basaltic dykes intrude the basement as well as the sedimentary succession. Towards the southeast, the basin comes into contact with the crystallines along the Senador Pompeu Lineament (SPL). The existing lithology and tectonic setting of the Parnaiba basin facilitate the formation of groundwater resource regions (see Meju et al, 1999; Chandrasekhar et al., 2005 and references there in). Integrated geophysical studies, viz., resistivity sounding, transient electromagnetic (TEM) and Audio magnetotelluric techniques for groundwater investigation have been effectively employed in some parts of Parnaiba basin (Meju and Fontes, 1996; Meju et al, 1999). Meju et al (1999) have also provided a quantitative estimation of the groundwater yield in the eastern margins of the Parnaiba basin. Chandrasekhar et al (2005) have analyzed magnetotelluric (MT) data and identified some pockets of groundwater resource regions in Guaribas and Caracol regions at shallow depths in Parnaiba basin.

Airborne magnetic data help to reveal presence of deep fractures, conducive for ground water accumulation. The targets are along major dislocations in the geology caused by faulting and shearing of rocks. Therefore, in the present study we attempt to check for the existence of any possible correlation between conductive zones in Guaribas region, mapped by MT data (Chandrasekhar et al., 2005) and causative magnetic anomaly sources in the study region using aeromagnetic data.

Aeromagnetic Data and Processing

High resolution three-component aeromagnetic data (X, Y, Z) and total field, F were collected along 41 parallel profiles oriented N28^{0}W at an altitude of 100m with an inter-profile spacing of 500m in Guaribas region by Fugro, in 2003. Fig.1 shows the schematic representation of airborne magnetic survey in Guaribas region. Cesium vapour airborne magnetic sensors of model CS-3 of Scientrex, having a sensitivity of 0.001nT have been used for recording data. Aeromagnetic total field anomaly map (Fig. 2) of the region obtained after correcting for the effects due to the main field shows several NW-SE structural trends within the basin proper. These structures are abruptly terminated at the NE-SW trending SPL.

Aeromagnetic Data Analysis: The Basin proper is composed mainly of shales, sandstones, quartz, and conglomerates etc, which are essentially non-magnetic. Hence the trends / structures visible in the aeromagnetic map reflect dykes or undulations / faults / fractures within the basement. The magnetic inclination and declination of the study region is -16.5^o and –21.7^o respectively and in low latitude regions a direct interpretation of the anomaly map can be erroneous (see Rajaram, 2003). Hence to get a better understanding of the distribution of magnetic sources, an analytic signal map (Roest et al, 1992) is used. The data were first upward continued to 500m to make them free from the high frequency (short wave-length) components. The resultant analytic signal map is shown in Fig.3, where red depicts magnetic sources. To locate the nature of the magnetic anomalies i.e., whether it is a fault or an intrusive or a three dimensional body, we have used the Euler's homogeneity equation (Reid et al,

1990). This equation relates the magnetic field and its gradient to the location of the source of an anomaly, with a certain degree of homogeneity expressed as structural index (SI). The SI is a measure of the fall-off rate of the field with distance from the source. For example an effective vertical line source, such as a narrow vertical pipe, gives rise to an inverse square field fall-off and an SI of two. We have calculated Euler's solutions for SI's ranging from 0 to 3. The best clustering of solution was obtained for SI = 0, which represents a fault / contact. Euler solutions have been calculated from the aeromagnetic anomalies as well as from the anomalies upward continued to 500m. The source depth and location of the Euler solutions obtained using the total field anomaly is superposed on Fig. 2 and the same obtained after continuing the anomalies upward to 500m is superposed on Fig. 3. In Fig.3, different coloured circles represent source depths of the Euler solution. The colour scale bar in Fig. 3 denotes the depth estimates of the Euler solution.

The aeromagnetic sources within the basin proper can possibly be related to the diabase dykes intruded into the basement as well as the sedimentary rocks. The present analysis suggests that the basement is traversed by several faults, which as a result has setup an environment favourable for ground water accumulation. The network of faults, interconnected underneath has been clearly brought out by the Euler solutions calculated from the upward continued data. These faults are buried under thick sedimentary cover. From analytic signal map (Fig. 3) it can be seen that the region 'A' is free from any major magnetic sources. It is bounded by NW-SE faults, which are cut by several small-scale NE-SW faults, thus forming potential zone for water conduits. The MT profile, AA' falls in this zone (see Fig. 1). The crystalline – sedimentary contact represented by SPL is evident in Euler solutions, showing up as major magnetic sources (Fig. 3).

MT Data Acquisition and Processing

MT soundings in the frequency range of 0.001-1000 sec. were made using EMI MT-1 equipment in April, 2003, along AA' laid perpendicular to the regional geological strike, the SPL. There are a total of 12 stations along AA' with an inter-station spacing of 1 km. MT data showed one-dimensional (1-D) characteristics at periods, ≤ 1 sec. Beyond 1 sec, the data are dominantly two-dimensional (2-D). We have modeled the data corresponding to the period range 0.01–10 sec. This is because at periods greater than 10 sec, the 2-D characteristics of data were not well resolved. We have processed MT data using the robust processing code of Egbert (1997). TEM measurements, made at each representative site, both in single-loop and in-loop configurations with loop length of 50m on each side, were used to correct static-shift effects in MT data wherever necessary (Jones, 1988; Sternberg et al, 1988) and rotated the impedance tensor to determine the optimum geoelectric strike angle using the algorithm of McNeice and Jones (2001). More details about data processing and procedure for strike angle estimation are given in Chandrasekhar et al (2005). The average strike angle for AA' is estimated to be -25^0 ($N25^0W$). The thus obtained geo-electric strike lies fairly parallel to the direction of the *local* geological strike, where there exist fragments of scattered small-scale faults and dyke-like structures, which are clearly seen in aeromagnetic data (Fig. 3).

MT Data Analysis: We have made 2-D inversion of fully constrained apparent resistivity and phase data of both TE (Electric field parallel to strike) and TM (magnetic field parallel to strike) modes simultaneously, with 10% (5%) of error floor on apparent resistivity (phase) data, using the non-linear conjugate gradients algorithm of Rodi and Mackie (2001). The model was iteratively derived until the combined (TE & TM) RMS error reached minimum. Fig. 4 shows the derived 2-D model for Guaribas (AA') region, shown up to a depth of 8km with an RMS error of 3.27. Derived model shows the best fit to TM mode data rather than to TE mode data. The best-fit between the observed and modeled apparent resistivity and phase data of TM mode is also shown on Fig. 4. Fig. 4 shows well defined high conductivity zones (marked as B1 and B2) located at depths of about 500m and 1000m at the SE and NW ends of AA' respectively. '**A**' represents the graben-like sedimentary basin structure. '*****' indicates the favourable location for drilling, for groundwater exploration in Guaribas region.

Discussion

Fig. 4 represents 2-D geo-electric model of the combined TE and TM data of AA' profile (see Fig. 1) with an RMS error of 3.27. Derived model clearly shows the Parnaiba basin to be very thin (maximum thickness of about 1000m in the study region) and conductive (resistivity of about 100-150 Ω-m). The model shows a sharp resistivity contrast between the sedimentary basin and the surrounding environment. The basin shows up as a thin sedimentary graben, with thickness of about 1000m-1500m in Guaribas region (marked as 'A' in Fig. 4). Model shows the basin being sandwiched between high resistive sedimentary rocks. Possibly, this could be due to the proximity of AA' profile to the regional geologic strike, the SPL, separating the sedimentary (in NW) and crystalline (in SE) regions, resulting in an inter-mixing of layered structures underneath. The derived model shows the best fit to TM mode data rather than to TE mode data. It is important to note here that the best fit of either of the modes to MT data essentially depends on the orientation of the existing subsurface structures, which control the polarization of the inducing field, which, in the present case, mostly favours TM mode rather than TE mode.

Two high conductivity zones (of resistivities <10 Ω-m), marked as B1 and B2 in Fig. 4 have been identified in Guaribas region. They are located at shallow depths of about 500m (SE end) and 1000m (NW end) in the sedimentary region. Primarily we believe that such high conductive zones are identified as fresh water sedimentary aquifers in sedimentary environment (see for e.g., Christopherson et al, 2002). The prevailing geology in the study area further supports our argument. B1 and B2 lie close to the faults identified from the Euler solutions (Fig.3). It is noteworthy that at both these locations the depths to the top of the fault (as estimated by the Euler solutions) are rather shallow and possibly formed a conduit for the water to percolate below. The top of these

faults lie at a depth of 150m and the identified conductive zones lie at a depth of 500m and 1000m respectively below these faults.

It is possible that the high conductivities of B1 and B2 (Fig. 4), could be due to the presence of dissolved minerals in them during the underground transportation of water from the neighboring Parnaiba river, flowing at a distance of about 300km NW from northern end of AA' profile through the meandering multitude of faults and fractures of the Trans-Brazilian Lineament. Secondly, there also exists a high yield Violeta fresh water well located at a distance of about 100km north of AA' profile.

As seen in Fig.4, although B1 is located at a shallow depth, drilling at this point may be difficult, as the mapped high conductivity zone is sandwiched between high resistive sedimentary rocks. However, it is worthwhile to explore B2, at the NW end of AA' profile (marked with '*' in Fig. 4), where drilling could be possible. At this point, not only the mapped high conductive zone is easily accessible through conducting sediments, but also it is located at a relatively shallow depth of about 1500m.

Conclusions

Analysis of high resolution aeromagnetic data collected over Guaribas region in Parnaiba basin has delineated several NW-SE faults, cut by small-scale NE-SW faults in the subsurface. MT soundings along selected profile have mapped high conductive zones at shallow depths, lying close to the ends of faults identified from aeromagnetic data. We believe that the mapped conductive zones represent sedimentary aquifers in the study region. Interestingly, at both the locations, where the conductors have been mapped, the depths to the top of the fault (as estimated from the Euler solutions) are rather shallow and possibly formed a conduit for the water to percolate below. This is supported by the presence of identified spouting and non-spouting wells near the study region. We recommend that this be confirmed by drilling, that could facilitate better assessment of water yield in this semi-arid region.

Acknowledgments

Part of the work was carried out, when one of the authors, EC was visiting Observatorio Nacional (ON) as a visiting scientist. He thanks CNPq for awarding him a visiting scientist fellowship. He thanks all the staff of ON for making his stay pleasant and comfortable and providing him with all the required facilities to carryout this work.

References

Chandrasekhar, E., Fontes, S.L and Flexor, J.M., 2005, Magnetotelluric Studies for Assessment of Groundwater Resources in Parnaiba Basin in Piaui State of North-East Brazil, (Communicated)

Christopherson, K.R., Jones, A.G. and Mackie, R., 2002, Magnetotellurics for natural resources: From Acquisition through interpretation, Soc. Explr. Geophys. Lecture notes, Salt Lake City, Utah, USA.

Cunha, F.M.B., 1986, Evolucao paleozoica da Bacia do Parnaiba e seu arcabouco tectonico: *MS thesis*, Univ. Federal Rio de Janeiro.

Egbert, G. D., 1997, Robust multiple station magnetotelluric data processing, *Geophys. J. Int., 130*, 475-496.

Jones, A. G., 1988, Static shift of magnetotelluric data and its removal in a sedimentary basin environment: *Geophysics, 53*, 967–978

McNeice, G. and Jones, A.G., 2001, Multisite, multifrequency tensor decomposition of magnetotelluric data, Geophys. 66 (1), 158-173.

Meju M., and Fontes, S.L., 1996, An investigation of dry water well near Floriano in northeast Brazil using combined VES/TEM/EMAP techniques, Proc. 8th EEGS symp. on application of Geophysics to Engineering and Environmental problems, 353-362.

Meju, M. A., Fontes, S. L., Oliveira, M. F. B., Lima, J. P. R., Ulugergerli, E. U. and Carrasquilla, A. A., 1999, Regional aquifer mapping using combined VES-TEM-AMT/EMAP methods in the semiarid eastern margin of Parnaiba Basin, Brazil, Geophys., 64 (2), 337-356.

Rajaram M,, 2003, Multi-Platform Imaging of Lithospheric Magnetic Anomalies, in: "The Indian Continental Lithosphere: Emerging Research Trends (Eds.) T.M. Mahadevan, B.R. Arora and K.R. Gupta", Memoir Geol. Soc. India, 53, 233 – 245.

Reid, A.B., Allsop, J.M., Granser, H., Miliett, A.J., and Somerton, W.I., 1990, Magnetic interpretations in three dimensions using Euler deconvolution, Geophysics. 55, 80-91.

Rodi, W. and Mackie, R.L., 2001, Non-linear conjugate gradients algorithm for 2-D magnetotelluric inversion, Geophys., 66, 174-187

Roest, W.E., Verhoef, J and Pilkington, M, 1992, Magnetic interpretation using 3D analytic signal, Geophys., 57, 116-125.

Sternberg, B. K., Washburne, J. C. and Pellerin, L., 1988, Correction for the static shift in magnetotellurics using transient electromagnetic soundings, Geophys., 53, 1459-1468.

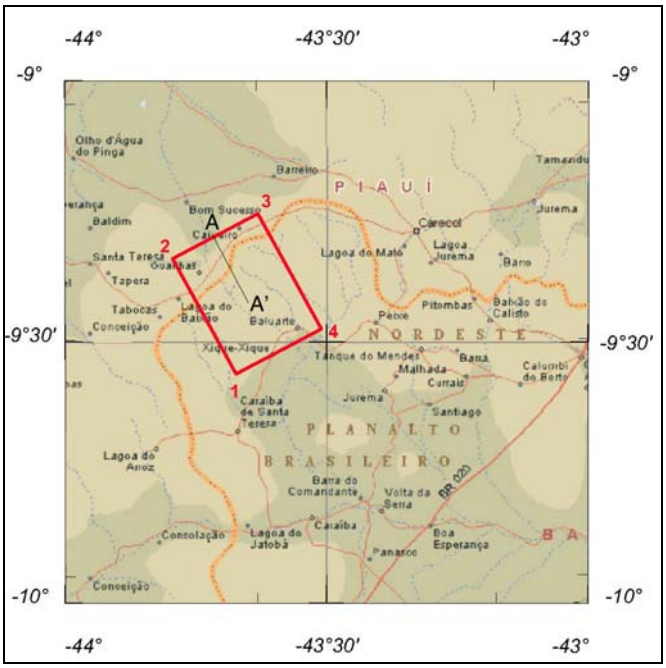

Fig.1. Schematic representation of the aeromagnetic survey area in Guariabs region in Parnaiba Basin (Red rectangle 1 2 3 4). AA' depicts the MT profile within the aeromagnetically surveyed region.

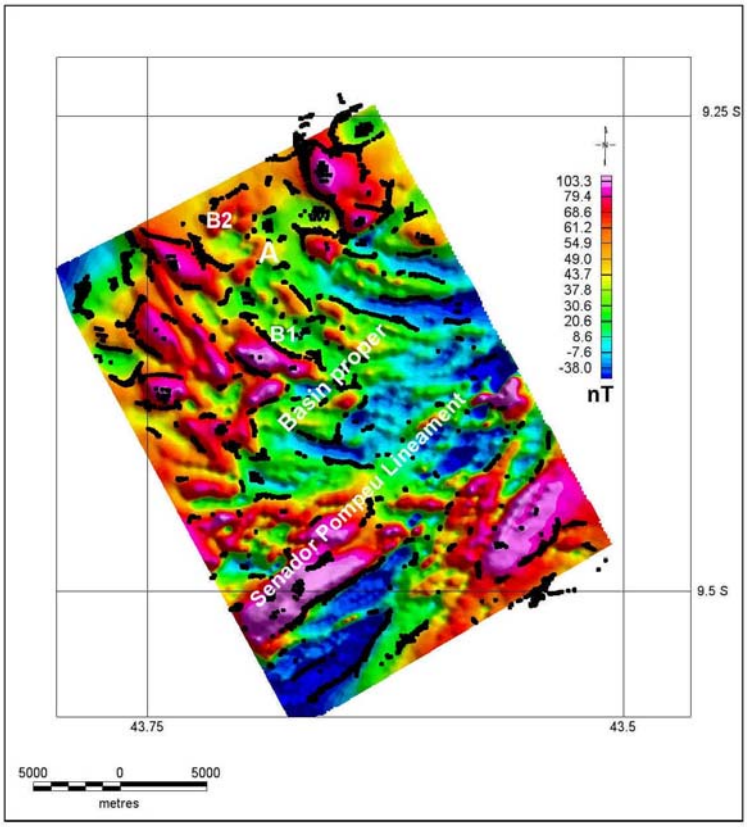

Fig. 2. Aeromagnetic total field anomaly map of the study region. Superposed on map are Euler solutions obtained from the anomalies. For explanation of B1, B2 and A, see caption of Fig. 3.

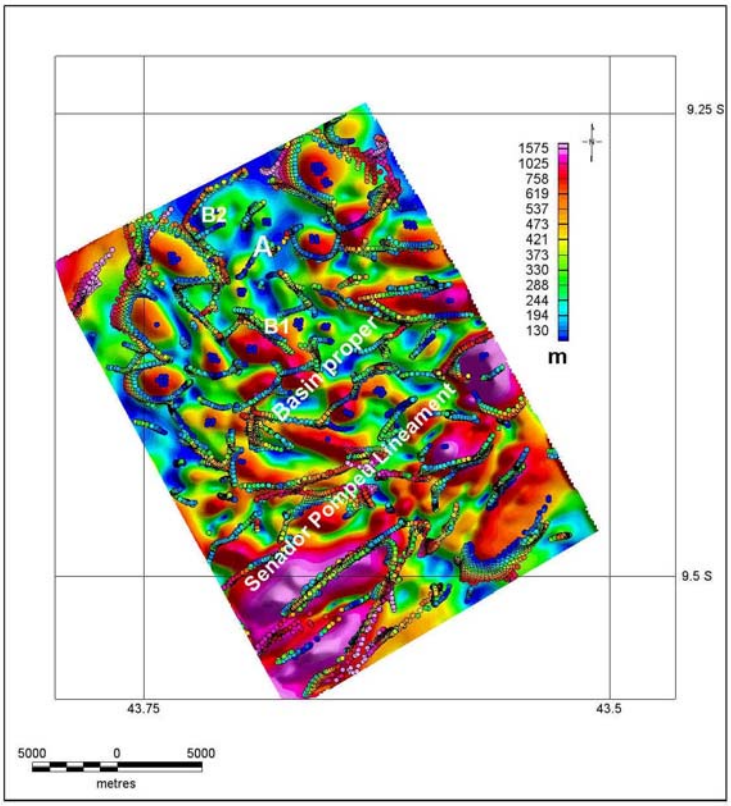

Fig. 3. Analytic signal map of aeromagnetic total field anomalies continued upwards to 500m. Red depicts the location of the magnetic sources. Superposed on the map are Euler solutions (coloured small circles) obtained from upward continued anomalies. B1 and B2 are from MT section (Fig.4). Region 'A' designates the zone relatively free from magnetic sources.

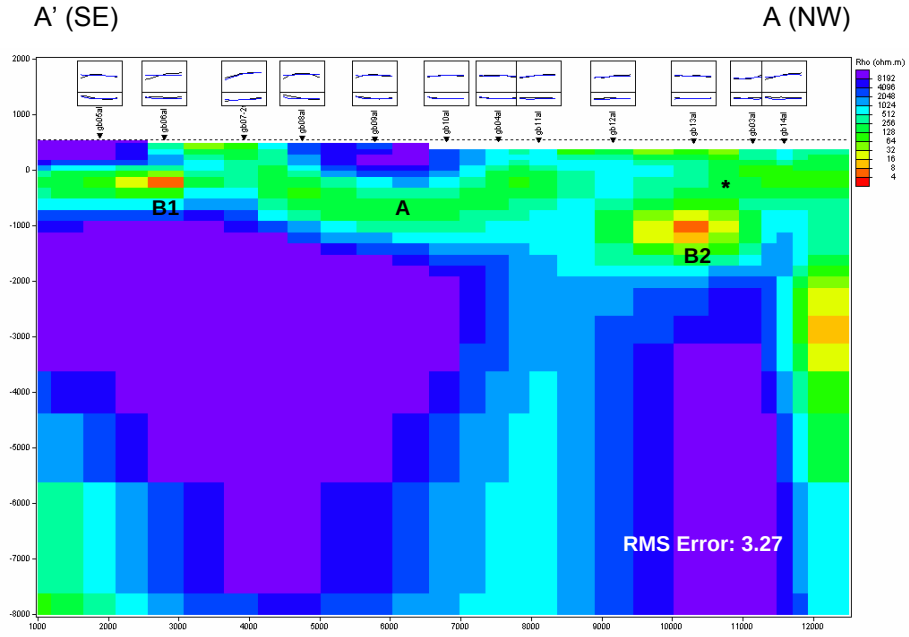

Fig. 4 Two-dimensional inversion model of MT data of Guaribas (AA') region. The rectangular boxes shown on top of the model represent the location of MT sites along the profiles as wells as TM mode fitting of apparent resistivity and phase data at respective stations. See text for description of labels on the model.